USE OF ANALYTICAL AND EXPERIMENTAL MONITORING TECHNIQUES IN ASSESSING THE PERFORMANCE OF A COLD REHEAT STEAM LINE

Chris Alexander
Stress Engineering Services, Inc.
Houston, Texas
chris.alexander@stress.com

Joe Frey, P.E.
Stress Engineering Services, Inc.
Houston, Texas
joe.frey@stress.com

ABSTRACT

After a catastrophic failure that occurred in a 30-inch diameter cold reheat (CRH) steam line at the W. A. Parish Plant, Texas Genco requested that Stress Engineering Services, Inc. (SES) assist in determining the cause of the failure. The incident occurred at approximately 12:10 PM on July 15, 2003 and resulted in a catastrophic failure that scattered components around the plant in a radius of 1,200 feet. Reliant Resources and Texas Genco conducted their own failure investigation that involved metallographic examinations, inspection of the fracture surfaces, review of operating conditions at the time of failure, and studies related to the weld profile of the CRH line.

Stress Engineering Services' efforts included studies using computational fluid dynamics (CFD) to address how droplet sizes from the attemperator might impact downstream behavior of the piping system. Follow-on work involved conducting a mock-up testing as well as field monitoring using high temperature strain gages, accelerometers, and thermocouples. The data obtained from the field monitoring efforts, along with process data provided by Texas Genco, were used to perform finite element analyses. The finite element work involved the calculation of static stresses as well as transient stresses generated by cycling of the attemperator (thermal stresses) and vibration of the line (mechanical stresses). Fracture mechanics was used to determine the times required for crack initiation and propagation to failure.

The analysis and monitoring efforts clearly demonstrated the operating conditions that were required to produce the failure. Additionally, the failure reinforced the importance of regular inspection of piping systems; even those high energy piping systems such as the cold reheat lines not normally associated with catastrophic failures.

INTRODUCTION

From the onset of the project, the focus was to determine the primary cause of the failure. Texas Genco and Reliant Resources had completed the bulk of their failure investigation prior to SES' involvement. Using an iterative process, efforts were undertaken to address the effects of the following potential contributors.

- Partially-plugged nozzle of the attemperator
- Size of droplets ejected with attemperator spray nozzles
- Stress concentration factor associated with internal weld profile
- Vibration of the piping system
- Quenching effects associated with cycling of the attemperator
- Performance of snubbers and spring hangers in vicinity of the failure

Failure Analysis Report

Initial efforts involved a failure analysis produced by Reliant Resources in their report (Shin, 2003). A brief description of the failure and background is provided here. At approximately 12:10 PM on Tuesday, July 15, 2003 a section of the W.A. Parish Unit #8 cold reheat line failed violently without any warning. Pieces from the failure were scattered over a radius of 1,200 feet. The attemperator liner launched from the vertical section of the piping. At the time of the failure the unit was operating at full load conditions with pressure and temperature being 685 psi and 675°F, respectively. At the time of failure the unit had approximately 145,000 hours of operation and had been re-rated in May 2001 from 660 psi/620°F to 685 psi/675°F. The seam welded cold reheat line was manufactured from ASTM A155, Grade KC70, Class 1 Carbon steel material. The dimensions were 30-in outside diameter by 0.636-inch minimum wall.
It is worth noting that there was nothing by review that would have caused this pipe to be included in an inspection program. It was well above minimum wall and was operated well below design.

Figure 1 and **Figure 2** are photographs from the Reliant Resources report that show the region where the failure occurred and a close-up view of the fracture surface. Of specific interest are the three fracture zones clearly shown in **Figure 2** and listed below.

- Region 1 (76% of wall) - initial smooth fatigue fracture zone
- Region 2 (16% of wall) - second rougher fatigue fracture zone
- Region 3 (8% of wall) - final overload fracture zone that failed on July 15, 2003

In reviewing the Reliant Resources report, the following key observations are made.

- Post-failure inspection revealed that failed region had an unground weld crown at the pipe inside diameter
- Failure occurred 41-ft downstream from the attemperator
- High cycle fatigue resulted from large number of relatively low amplitude stresses (such as those from attemperator cycling)
- The Reliant Resources report states that attemperator cycling likely source of cyclic stresses

Engineering Analysis, Testing, and Monitoring Work

This section outlines the efforts of SES in working with Reliant Resources to determine which factors played a critical role in the cold reheat line failure and the ranking for those contributors. To accomplish this, the following methods and techniques were employed:

- Flow analysis of attemperator using computational fluid dynamics
- Full-scale mock-up testing of attemperator using pressurized water
- Piping stress analysis using the CAESAR II piping software
- Detailed analytical efforts using finite element methods to address
    - Stress concentration factor (SCF) due to weld profile
    - Thermal transients (quenching of attemperator)
    - Piping distortion and displacement due to thermal expansion and pressurization near elbow
    - Effects of manufacturing ovality
- In situ monitoring to assess temperature profile, strains, and accelerations
- Analysis to address vibration of the line considering flow-induced excitation

Another important element of the work performed considered the type of loads and operational history of the CRH line. The loading due to cold start-ups, normal shut-downs, hot restarts, daily pressure load cycles, cycling of the attemperator, and vibration were included. Stresses were computed for each load type and the cumulative damage was assessed by summing the individual stress-cycle combinations. A fatigue assessment and fracture mechanics evaluation was then performed to verify the potential for failure. The analytical results clearly indicate crack initiation and propagation to failure.

The sections that follow provide additional details on the SES methodology and techniques used in performing this investigation. A presentation is also made detailing the methods and results of the fatigue analysis and cycles to failure considering fracture mechanics. To finish the discussion, a summary chapter is provided that ranks the contributors to failure.

COMPUTATIONAL FLUID DYNAMICS ANALYSIS

Computational Fluid Dynamics (CFD) techniques were applied to simulate the thermal and fluid behavior in the cold reheat pipe and to study the evaporation and transport of quench spray in the reheat pipe. In normal operation, the steam in the cold reheat line is quenched by spraying water in the attemperator section. The objective of this work was to examine the transport of quench spray in the reheat pipe.

The cold reheat line consists of the attemperator and the associated piping that carries the steam. The region of interest is depicted in **Figure 3**. The geometric details of the attemperator nozzle itself are not modeled. A spray of water is initiated at the nozzle location and the resulting flow field is studied in detail.

CFD simulation was applied to examine the flow behavior in the CRH line. The influence of water spray flow rate and water droplet size on the flow and thermal behavior in the cold reheat line is examined. **Figure 4** through **6** show the distribution of the flow considering water droplets with diameters of 0.1 mm, 1 mm, and 10 mm. The selection of droplet size was based on an effort to reasonably bound the problem, as opposed to actually measured values.

The results indicated that larger droplets (10 mm) impinge on the walls of the attemperator; whereas smaller droplets (0.1mm) are carried by the flow. Droplets of an intermediate size (1mm) evaporate in the vertical section while the droplets of reduced size (0.1) impinge near the first elbow. Local temperature variations due to impingement of droplets are observed. Another important observation concerns the appreciable temperature variation (30 K, 54 F) is observed in the elbow region due to variations in the quench water flow rate when the 1 mm droplets are injected as shown in **Figure 7**. This variation in temperature suggests a possible mechanism for failure of the line. Finite element analysis was used to address the influence of temperature variation induced by quench water flow rate on the structural behavior of the CRH line. The results of the finite element analyses are reported separately.

MOCK-UP TESTING

During the failure investigation of the CRH line by Reliant Resources partial plugging of one of the attemperator nozzles was observed. There was concern that this plugged nozzle contributed to the failure of the line. For this reason, Texas Genco requested that a full-scale mock-up test be conducted.

The primary objective of the mock-up testing was to determine if any significant water spray pattern irregularities developed (including the development of large water droplets).

The following observations were made directly by viewing the high speed and high definition videos as shown in **Figure 8**.

- The partially plugged nozzle did affect the exit angle of the water spray as it left the attemperator nozzle (note the differences in the water ejection angles when comparing the unplugged and partially-plugged nozzles shown in **Figure 8**)
- Even at 2,000 frames per second, the video showed no sizable water droplets were observed when exiting the partially plugged nozzle.

The mock-up testing played an important role in validating that the partially plugged nozzle did not significantly affect the attemperator spray. While there was an effect on the exit angle of the water spray as it left the attemperator nozzle, the high speed video showed no sizable water droplets when exiting the partially plugged nozzle.

ON-LINE MONITORING OF UNIT #8

Electronic measurement devices were installed on the replacement pipe (combination of welded and seamless) to monitor temperature, vibration, and strain in the CRH line upon its return to service. The equipment was installed at select locations downstream of the attemperator. Stress Engineering Services studied the drawings and process data provided by Reliant Resources and Texas Genco for the CRH line to determine sensor placement. The region of focus centered between the attemperator and where the failure occurred, although sensors were placed upstream of this location. The following sensors were used to make measurements at selected locations.

- High temperature strain gages
- Thermocouples used to measure localized temperatures
- Accelerometers used to measure vibration (acceleration)

Figure 9 provides a schematic diagram showing where the instrumentation was installed. **Table 1** provides additional details on the specific types of equipment that were installed at each location. Due to the elevated temperatures (above 500°F) associated with the CRH line, high temperature strain gages were required.

In addition to the sensors, a laptop computer and data acquisition system were used to collect data. The data acquisition system permits the recording of data at selected scan rates (e.g. 200 scans per second). The Stress Engineering Services StrainDAQ system was used for collecting and processing the measurement data.

Once the equipment was installed, data was recorded at the following rates.

- Long-term monitoring - data recorded every 5 seconds (0.2 scans per second) and was useful for looking at trends over several hours and days
- High speed data collection - data recorded at a rate of 200 scans per second and was useful for looking at short bursts of data such as information associated with vibration

Data was collected at several different times during the course of a three week period. Although a large amount of data was collected, only data that contributed to key observations is presented here.

Collection of Temperature Data

The primary purpose of the attemperator is to control the temperature of the steam that enters the boiler. The failure in the CRH line occurred approximately 41 feet downstream of the attemperator. The CFD efforts demonstrated that with smaller water droplets (0.1 mm) and high steam flow rates (65,000 lbs. per hours) the temperature in the failure region could be reduced. This temperature drop is significant in that it contributes to generate thermal stress transients. The attemperator was cycled approximately 300,000 times prior to the failure (50 cycles per day over 6,000 days). **Figure 10** shows temperature data that were recorded during a three and a half hour period that included one (1) attemperator cycle. As noted in this figure, there is a localized temperature drop that occurred when the attemperator started to cycle.

It is important to note that this data represents external pipe temperatures. The highest thermal stress in the region of the failure occurs on the inside surface of the pipe at the weld. As the attemperator cycles on, relatively cold fluid impacts the inside surface of the pipe and reduces the inside surface temperature. Because of the reduced temperature, the inside surface attempts to contract but is restrained by the outer region of the pipe that is at a higher temperature. The resulting tensile stresses on the inside surface of the pipe are detailed elsewhere in this report.

Collection of Stress and Strain Data

The collection of stress data involved long-term and high speed data acquisition rates. Elastic stresses are computed from the strain gage readings and compensated to account for elevated temperatures. The long-term data was useful for developing an understanding about how the cycling of the attemperator affects stresses, while the high speed data was useful for providing insights about the frequency and range of stresses associated with the high speed vibration data. The high speed required post-computation analysis using rainflow cycle counting techniques.

Figure 11 shows hoop stress measurements for the same period associated with the temperature data plotted previously. During the time before the attemperator is turned on the hoop stress on the outside surface is about 12.0 ksi. A significant drop in the measured tensile stress occurs on the outside surface of the pipe when the attemperator cycles. As discussed previously, a tensile load is generated on the inner surface of the pipe, while a compressive load occurs on the outer surface due to the through-wall temperature differential. This loading is superimposed on top of pressure loads that create the hoop stress.

Closing Comments on Measurement Work

Results for the monitoring efforts have been presented. When used in conjunction with the analytical stress results, the field data provide important observations about how the cold reheat line performs. This is especially important when considering the transient responses associated with the attemperator cycling. The temperature drop in the region of the elbows not only confirms the analytical CFD work, but also validates that stresses in the line are generated by the quenching process that occurred approximately 300,000 times prior to the failure.

STRESS ANALYSES

The sections that follow provide specific details on the finite element models that were used in the analytical efforts. The following models were considered.

- CAESAR II model (beam element model used to calculate general stresses used in design)
- ABAQUS global model (used a combination of beam and shell elements to capture general stresses in the area of the failure)
- ABAQUS plane stress model (used two-dimensional continuum elements to calculate the stress concentration factor in the weld region subject to internal pressure)
- ABAQUS transient plane stress model that also included ovality (used two-dimensional continuum elements to calculate stresses associated with the transient quench of the attemperator)

CAESAR II Design Model

Reliant Resources provided to SES an input file for a CAESAR II model and requested that additional information be obtained from the model. Minimal information on the CAESAR analysis is presented in this paper; however, one of the primary objectives in the request from Texas Genco for the piping analysis was to assess the performance of the snubbers and what happened if the one nearest the failure (H14) was not working properly. Based upon details provided in the Reliant Resources drawing package, the snubbers were sized for a maximum load of 10,000 lbs. The CAESAR modeling efforts showed that snubber loads typically exceeded 15,000 lbs, indicating that even if the snubbers were functioning correctly (they were not as the snubber provided no resistance), there is the potential that they were overloaded, especially the one closest to the failure (snubber H14).

Shell and Beam Global Model

While the CAESAR II model was useful for calculating design stresses, it did not permit detailed stress calculations involving geometric deformations such as ovality. To do a more detailed study of the original design, an ABAQUS finite element model was constructed. ABAQUS is a general-purpose finite element code that can be used to solve a variety of technical problems including structural and heat transfer analyses. **Figure 12** shows the basic framework for the finite element model that incorporated beam and shell elements. The region of interest (where the failure occurred) is modeled using shell elements. It is sufficient to model other regions of the piping system with beam elements. The beam elements have the appropriate stiffness and ensure that the piping in the failed region is loaded correctly in terms of applied forces, torques, and bending moments.

The model incorporated the following load combinations.

- Spring hanger loads and cold spring
- Gravity

- Internal pressure of 685 psi
- Isothermal temperature of 675°F

Each of the above four loads was applied in an additive manner. In other words, once the thermal load was added the calculated values (e.g. stress, displacement, etc.) included all loads. In terms of post-processing, the two most useful pieces of information included the following.

- Stress in the vicinity of the failure. The calculated stress included the effects of pressure and thermal loading, and also integrated the effects of the elbow adjacent to the failure.
- Local displacement and ovality induced in the vicinity of the failure. Although the shell model provided membrane and bending stresses, it does not accurately represent stresses generated in the weld region.

Figure 13 shows makeup, gravity, pressure, and temperature loading, while **Figure 14** provides a close-up view of the piping in the vicinity of the failure. As noted in this figure, high stresses developed in the failure region and will be even higher than calculated with the shell elements when integrating the weld stress concentration factor.

The general observations associated with the shell and beam model are as follows.

- Stress in pipe where the failure occurred adjacent to the elbow is on the order of 15,000 psi (0.780-in pipe wall)
- Shell and beam model does not address stress concentration due to weld profile
- Stress in pipe due to bending loads is generated by thermal and pressure loads
- Shell and beam model only considered isothermal loading at 675°F and internal pressure of 685 psi

Building upon the lessons learned with the shell and beam model, additional work was conducted to calculate detailed stresses in the vicinity of the weld. For this task, a plane stress model was selected.

Plane Stress Model

To determine peak stresses in the vicinity of the weld, a plane stress model was constructed. The geometry for this model was based upon detailed measurements obtained from the Reliant Resources failure analysis report. **Figure 15** shows a close-up of the stress contour plot in the region where the failure initiated. As noted, a SCF of 4.35 is calculated considering the pressure-only stress. This figure shows a cross-section of the weld crown in the region where the failure occurred. In the absence of an actual root radius in the weld toes, a radius of curvature equaling 0.005-inches was used at both locations.

The predominant observations from the plane stress model that considered pressure-only loading are as follows.

- Plane stress model used to calculate stress concentration factor associated with weld
- Weld geometry taken from Reliant Resources failure report (scaled from photo)
- Loading generated by internal pressure
- Ovality levels of 0.5 and 2.0 percent pipe outer diameter considered
- Analysis also considers ovality induced by loads from global model

Transient Plane Stress Model

Due to concerns that the transient thermal stresses were key contributors to the CRH failure, a transient plane stress model was analyzed. The following progressive steps to a transient response were observed.

1. Prior to cycling of the attemperator, the cold reheat piping is at a relatively constant temperature. This was observed in the area where the failure occurred.
2. Once the attemperator starts to cycle, cold fluid is injected into a steam flow. Water droplets within this now-combined flow continue downstream where they reduce the overall temperature of the mixture as well as the piping.
3. The transient temperature effects take place when the hot wall is impacted with the cooler steam (including water droplets from the attemperator). The inner surface of the pipe wall attempts to contract due to the reduced temperature, but is prevented from doing so by the outer region of the wall that is still at a higher temperature. This results in generating tensile loads on the inner surface of the pipe. Conversely, the outer surface of the pipe will initially show compressive loads. These loads are superimposed on top of the existing pressure and static thermal loads.
4. At some point the steady-state condition returns and the pipe once again exists at a relatively isothermal state.

Stress Engineering Services modeled the transient response of the pipe subject to the aforementioned conditions, with specific emphasis on calculating stresses in the toe of the weld where the failure occurred. **Figure 16** shows the transient thermal stresses as a function of the internal skin temperature. When the internal skin temperature is 520°F the transient stress range is 138.4 ksi, whereas when the internal temperature is increased to 640°F the transient stress range is only 36.2 ksi.

In reviewing the results and trends associated with the transient plane stress model, the following observations are made.

- The injection of the cooler fluid into the pipe generates a quenching effect on the inside pipe surface
- Field data show that temperatures vary along the length of the piping system upstream of the area of interest
- Significant tensile stresses are generated in the vicinity of the weld
- Stresses exceeding the yield strength of the material are generated in the weld area during some thermal transients
- The quenching effect is cyclic (approximately 300,000 cycles in 145,000 hours of operation)

FATIGUE AND FRACTURE MECHANICS

For a system subjected to cyclic service, such as the CRH line, an engineering failure assessment must consider fatigue. The cycles to failure for a given stress range is used as input in performing a cumulative damage assessment. Using this technique it is possible to demonstrate that a fatigue fracture can initiate given enough cycles having sufficient stress ranges. The attemperator operation generated stresses that were of sufficient magnitude and frequency to initiate a crack in the longitudinal weld seam. Once there was sufficient cyclic loading for crack initiation, a fracture mechanics evaluation was performed to estimate the required cycles to failure. It should be noted that the photomicrograph (Shin, 2003) showed oxide scale at the beginning of the crack of the same thickness as the scale on the ID surface immediately adjacent to the crack. This report states that the crack initiated early in the service life of the pipe.

Appendix 5 of the ASME Boiler & Pressure Vessel Code, Section VIII, Division 2 (Code) provides procedure for performing a fatigue evaluation for structures subjected to cyclic service. The methodology

presented in Appendix 5 (and even the design curves) has been used on many applications other than just pressure vessels. Division 3 of the Code also includes design fatigue curves and includes curve fits for the different curves. Although the use of the published ASME curves is appropriate for design, these curves are not appropriate for predicting cycles to failure unless the underlining design margins are removed. The design fatigue curve selected from Division 3 is based upon Figure KD-320.2 which is for welded components made from carbon or low alloy steels with an ultimate tensile strength less than 80 ksi. This design curve was modified by removing the design margin on stress and cycles as well as extending the range beyond 10^6 cycles at the same slope as the curve for less than 10^6 cycles. This removes the inflection point and associated endurance limit of the curve at 10^6 cycles. The curve fit for this line is given by the following equation.

$$N = \exp(-2.8342 \cdot \ln(\sigma_a/2) + 19.7046) \quad (1)$$

Where σ_a is the stress amplitude for the given load cycle (one-half of the stress range). For elevated temperatures, σ_a must be multiplied by the ratio of modulii based upon elastic modulus at room temperature divided by modulus of elasticity at the elevated temperature. At 675°F, the elastic modulus is 25.8 x 10^6 psi. It should be noted that the calculated number of cycles in this way actually corresponds to cycles to crack initiation for the mean of the material fracture data. This is an important point, especially as it relates to understanding the role that fatigue evaluation and fracture mechanics play in determining the estimates time to failure.

Table 2 provides a summary listing of the calculated stress ranges for the load combinations that were assumed to contribute to the cold reheat line failure. Also included in this table are the estimated cycles to failure using the ASME-modified fatigue curve and the cumulative usage factor, U. The cumulative usage factor is calculated by dividing the actual applied number of cycles at that respective stress range, n, by the calculated cycles to failure, N.

DISCUSSION

The following factors were deemed to have contributed in some fashion to the failure of the cold reheat line (listed in order of criticality). Note the use of the designations ***primary/secondary*** and ***tertiary***.

1. Stress concentration factor associated with internal weld profile – **primary/secondary contributor**
2. Location of failure relative to elbow– **primary/secondary contributor**
3. Quenching effects associated with cycling of the attemperator– **primary/secondary contributor**
4. Vibration of the piping system– **tertiary contributor**
5. Performance of snubbers and spring hangers in vicinity of failure– **tertiary contributor**
6. Size of droplets ejected with attemperator spray nozzles (could contribute if flashing develops) – **tertiary contributor**

CONCLUSIONS AND CLOSING COMMENTS

This report reflects a significant amount of work involving Reliant Resources who was contracted by Texas Genco, SES, EPRI, and EMT. Without contributions from all participants, completion of this project would have been difficult. Reliant Resources's failure report provided the foundation for the SES work that included CFD modeling, mock-up testing, in situ field monitoring, and detailed stress analyses. The fracture mechanics assessment provided by EMT provided verification that crack propagation could take place within one lifetime and that Stress Engineering's stress calculations were sufficient to initiate a crack that would lead to an eventual failure.

What has been demonstrated in this work is how a failure investigation can be coupled with testing, monitoring, and analyses to not only determine causes of failure, but specific steps that can be taken to prevent future failures.

For industry there are some important lessons to be learned from Texas Genco's failure. The first and primary lesson relates to the stress concentration factor associated with the internal weld crown. Had this weld crown not existed and been ground smooth like other weld areas in the pipe, it is highly unlikely that the failure would have occurred. Secondly, because the cracks more than likely initiated after commissioning, there is sufficient evidence to warrant the periodic inspection of all welds. For piping systems with over 100,000 hours of service and a high number of accumulated attemperator cycles, weld inspections should be conducted. Thirdly, industry standards and codes should require that all seam-welded pipes have their longitudinal welds ground flush to reduce the potential for fatigue damage. Lastly, each operator should have a thorough understanding about how the attemperator affects thermal quenching, especially when in close proximity to elbows or other complex piping arrangements.

Vibration in the new piping system has been reduced by the modified support system and upgraded piping hangers. Additionally, the CRH line is now part of the high energy piping inspection program (it was not before the incident), These two observations contribute to the future long-term success that is likely for the Unit #8 CRH line.

By integrating the important lessons learned in this study for Texas Genco, the power industry can ensure the safe operation of its cold reheat lines and reduce the potential for catastrophic failures based upon observations and sound engineering.

REFERENCES

ASME (2001), 2001 ASME Boiler & Pressure Vessel Code, Section VIII, Division 3, *Alternative Rules for the Design of High Pressure Vessels*, The American Society of Mechanical Engineers, New York, New York, 2003 Addenda, July 1, 2003.

ASME (2001), 2001 ASME Boiler & Pressure Vessel Code, Section VIII, Division 2, *Alternative Rules*, The American Society of Mechanical Engineers, New York, New York, 2003 Addenda, July 1, 2003.

Blevins, R.D. (2001), *Flow Induced Vibration, Second Edition*, Krieger Publishing Company, Malabar, Florida, 2001, pages 384-392.

Harris, D.I. (2003), *Analysis of Fatigue Crack Initiation and Growth in Parish Unit 8 Cold Reheat Line*, Engineering Mechanics Technology, Inc., San Jose, California, December 5, 2003.

Pikey, W. D. (1997), *Peterson's Stress Concentration Factors, Second Edition*, John Wiley & Sons, New York, 1997, pages 36-40.

Shin, S. (2003), *Metallurgical Analysis of Cold Reheat Pipe Failure at WA Parish Station Unit 8*, Reliant Resources Report from Central Technical Services, Reliability Engineering, October 6, 2003.

Figure 1 - Horizontal spool piece showing fatigue-cracked seam weld

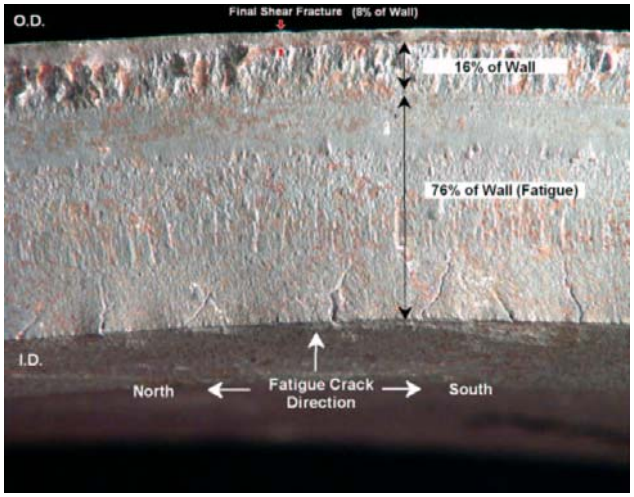

Figure 2 - Close-up view of fracture showing distinct fracture zones

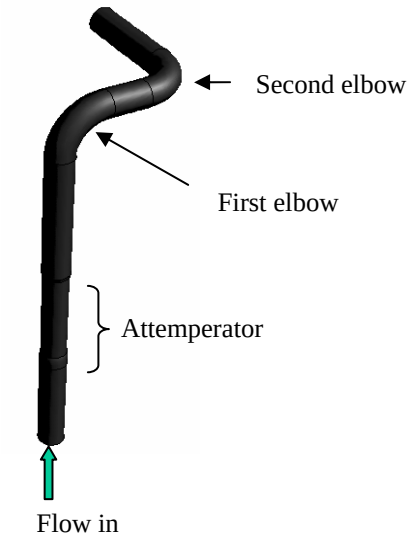

Figure 3 - Flow domain for the CFD model

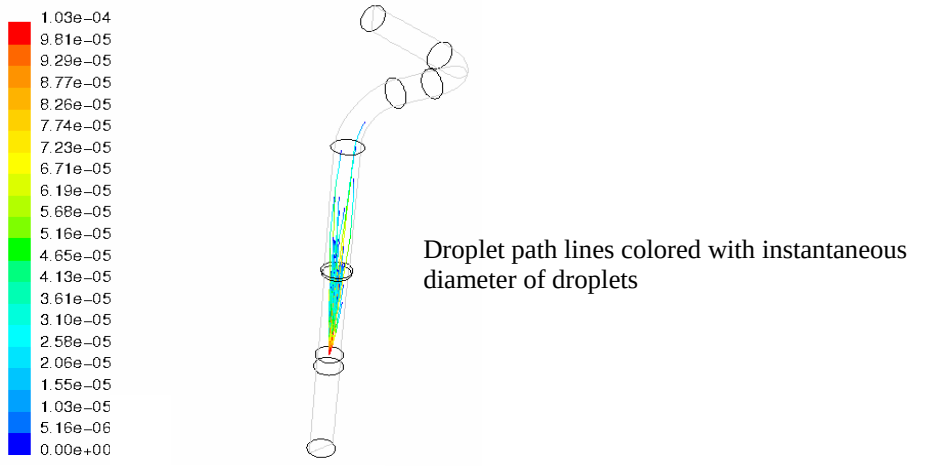

Figure 4 - Droplet path lines with 0.1 mm droplet diameter at injection

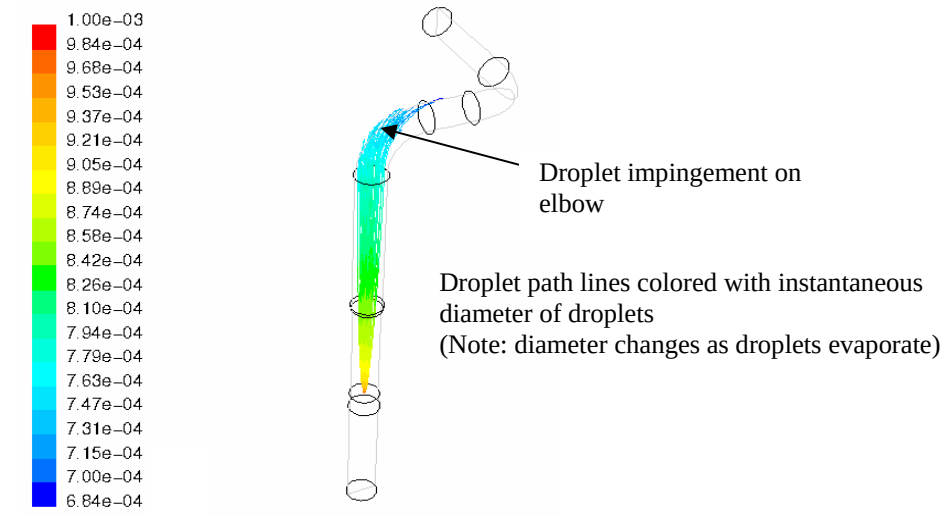

Figure 5 - Droplet path lines with 1 mm droplet diameter at injection

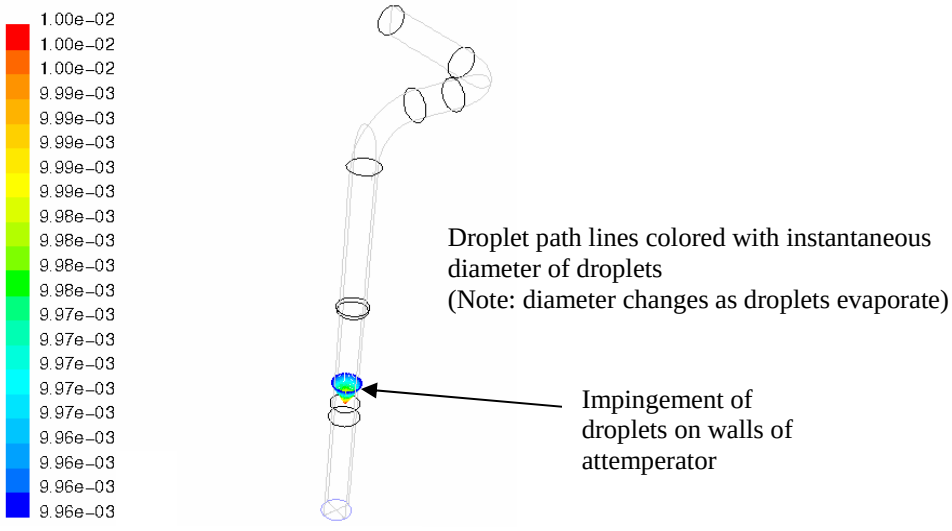

Figure 6 – Droplet path lines 10 mm droplet diameter at injection

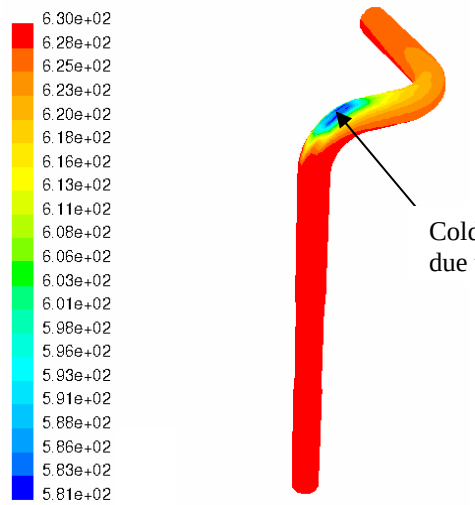

Temperature (K) (630K=675F, 1K difference=1.8F difference)

Figure 7 - Surface temperature distribution on pipe with 1 mm droplet

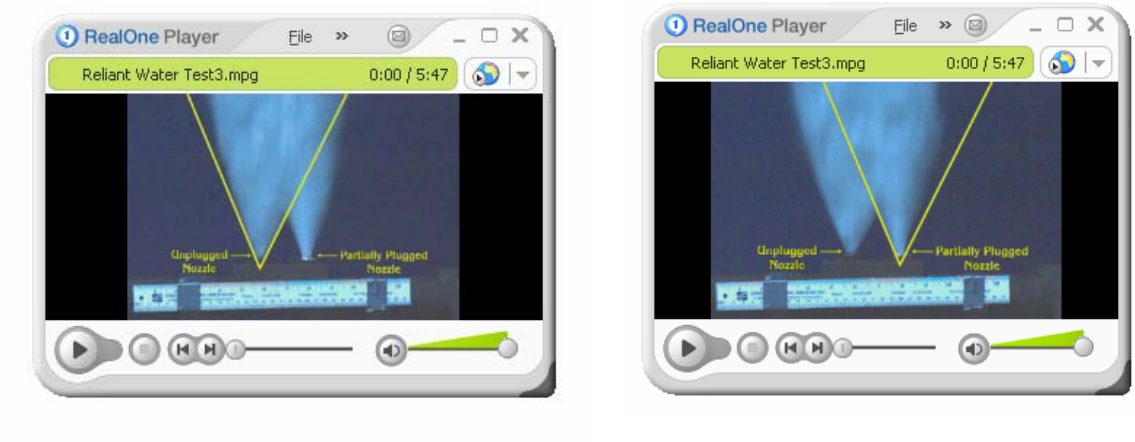

Figure 8 - Images from high speed filming at 2,000 fames per second
(Unplugged nozzle on LEFT and partially-plugged nozzle on RIGHT)

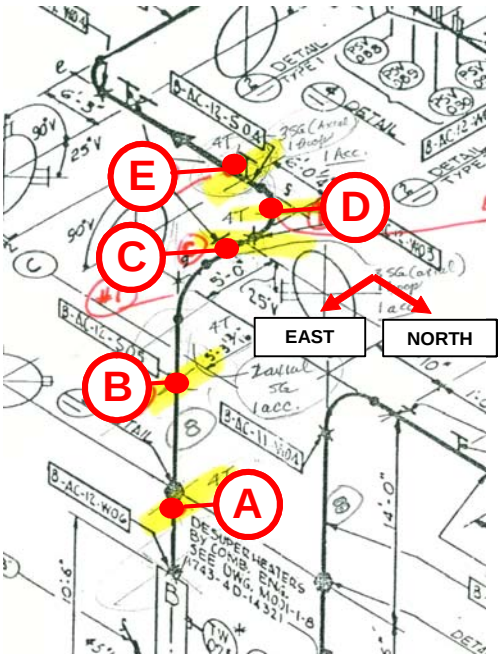

Figure 9 – Locations A through *E* for electronic equipment

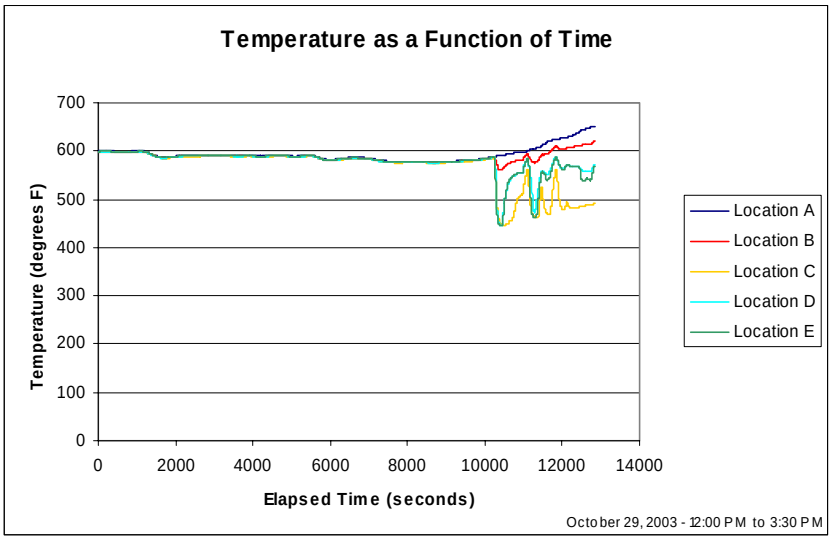

Figure 10- Temperature at selected locations over a 3-1/2 hour period

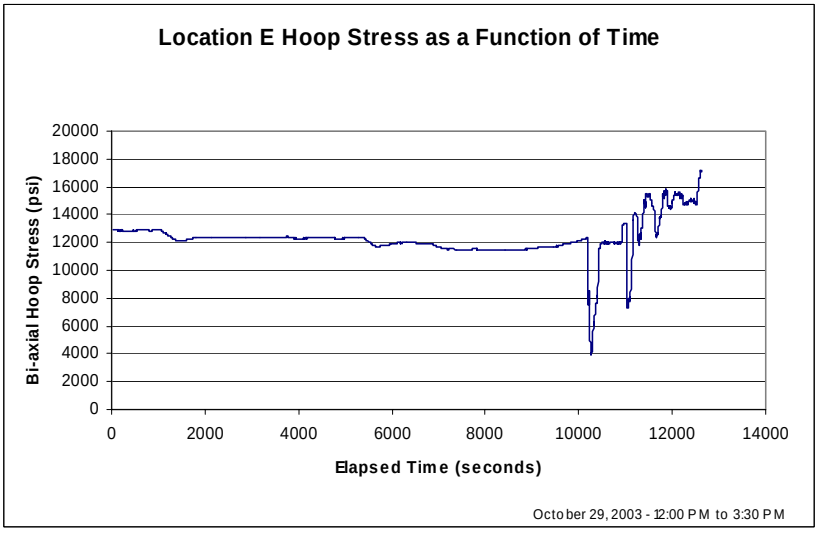

Figure 11- Hoop stress recorded near failure region

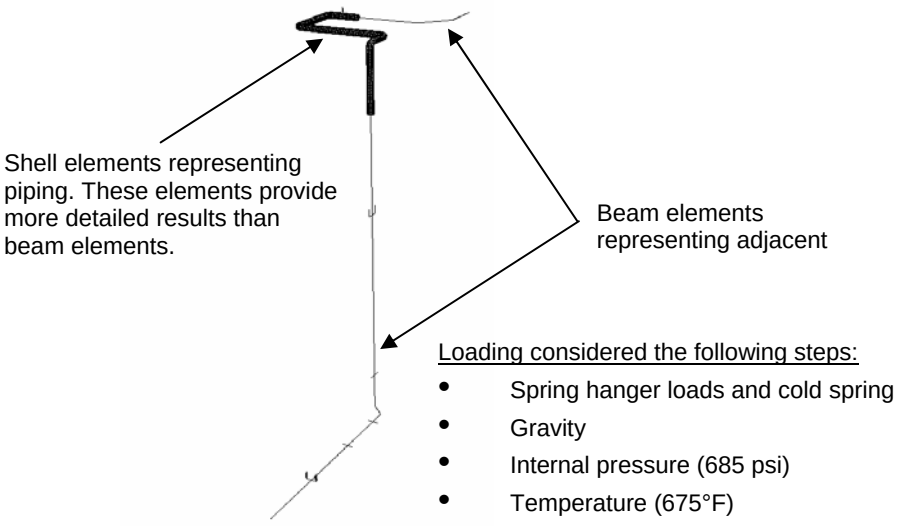

Figure 12- Global model including beam and shell elements

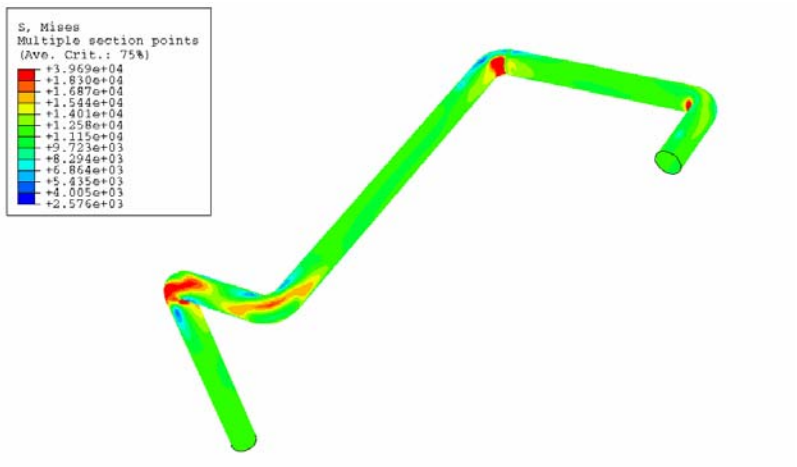

Figure 13 - Von Mises Stress contour plot with makeup, gravity, pressure, and thermal loading

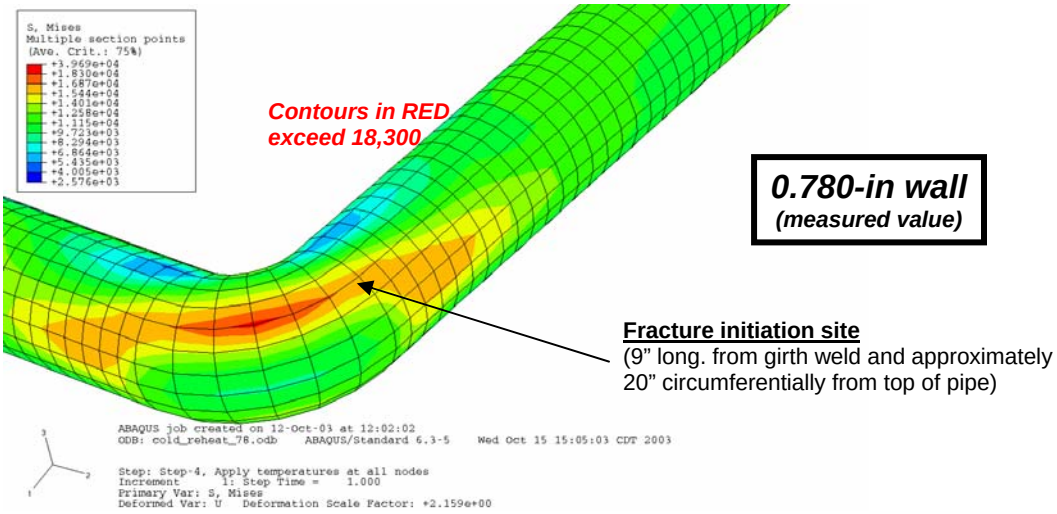

Figure 14 - Close-up view of stresses in the vicinity of the failure

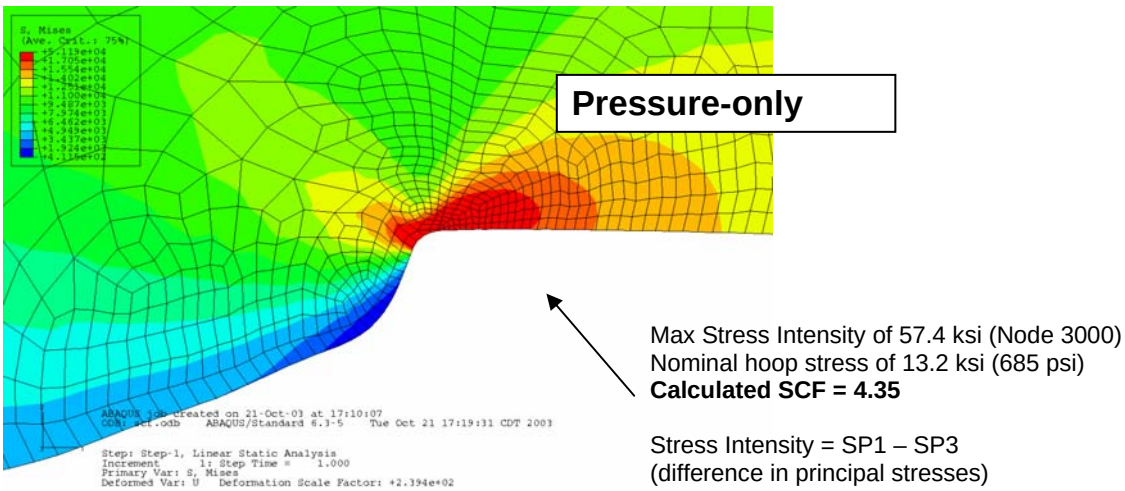

Figure 15 -Detailed stress contour plot including SCF value

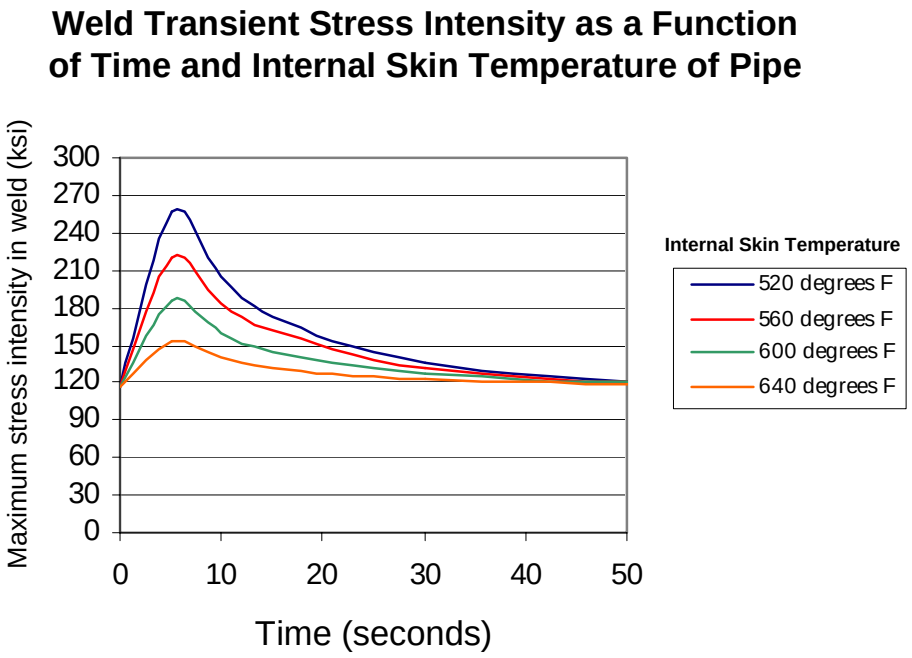

Figure 16 - Transient stresses as functions of internal bulk temperature

Table 1 - Number and type of electronic sensors

Location A	Location B	Location C	Location D	Location E
3 TC	3 TC	3 TC	3 TC	3 TC
	3 ACCEL	3 ACCEL	3 ACCEL	3 ACCEL
				4 HTSG

Notes:
Refer to **Figure 9** for instrumentation locations
TC – thermocouple
ACCEL – piezoelectric accelerometers
HTSG – high temperature strain gage – three (3) axial gages and one (1) hoop gage

Table 2 - Stress Ranges for Operating Load Combinations

Operating Condition	Stress Range σ_r ksi	Cycles to failure, N	Applied operating cycles, n (4)	Usage Factor n/N
Cold start-up (considers pressure, temperature, and attemperator quench)	275.8 (1) ***188.2*** (2)	1,564 ***4,619***	55	0.0352 ***0.0119***
Hot start-up (considers temperature and attemperator quench)	159.9 ***130.8***	7,330 ***12,953***	180	0.0246 ***0.0139***
Daily pressure fluctuation (ΔP= 350 psi)	59.2 ***29.3***	122,504 ***899,224***	6,000	0.0489 ***0.0067***
Attemperator cycling (T_{inside} = 560°F)	103.6 ***74.5***	25,080 ***63,856***	300,000	1.0 (3) ***1.0***
Vibration	4.2	221.2 x 10^6	26.1 x 10^6	N/A

Notes:
(1) Calculated stress results assume ovality due to manufacturing of 2.0 percent.
(2) Values in ***bold italics*** correspond to data for pipe with 0.0 percent ovality.
(3) Any value of U that exceeds unity (1) indicates that crack initiation is possible for 50 percent of the material based upon statistical variances.
(4) These applied operating cycles are in the 145,000 hours of service that preceded the failure